Removal of Methylene Blue, Malachite Green and Rhodamine B in a Ternary System by Pistachio Hull; Application of Wavelet Neural Network Modeling and Doehlert Design

Reza Tabaraki*, Ashraf Nateghi

Department of Chemistry, Ilam University, Ilam, Iran
(Received 2 October 2017, Accepted 15 January 2018)

Most of previous papers in the field of dye removal used one dye or dyes with nearly separate spectra simplifying dyes concentration determination by Beer's law at different λ_{max}s. In many real situations, dyes with highly overlapped spectra exist and their concentrations can be determined by multivariate analysis methods. In this study, principal component-wavelet neural network (PC-WNN) was used for concentration determination of rhodamine B (RB), methylene blue (MB) and malachite green (MG) in ternary solutions. Biosorption of dyes by pistachio hull was selected as model. The effects of operating parameters were studied by Doehlert experimental design. The maximum uptake capacity of pistachio hull for cationic dyes was 0.682 mmol g^{-1}. It was found that the overall biosorption data was described by the pseudo second-order kinetic model. Nine isotherm models were nonlinearly fitted to experimental data and Redlich-Peterson and Radke-Prausnitz isotherm models had the best fit for biosorption equilibrium data.

Keywords: Cationic dyes, Nonlinear fitting, Doehlert design, Wavelet neural network, Isotherm

INTRODUCTION

Dyes are synthetic organic compounds used as colorants in textile, leather, plastic and paper industries [1]. There are more than 100,000 commercial dyes with an estimated production of 7×10^5-1×10^6 tons/year worldwide. It is estimated that 10-20% of dyes are lost during the manufacturing and dyeing processes and produce large amounts of dye-containing wastewater [2,3]. The dye-containing wastewater can adversely affect the aquatic environment by impeding light penetration. Moreover, most of the dyes are toxic, carcinogenic and harmful for human health [4]. Therefore, the treatment of dye wastewaters and finding dye-removal efficient methods have been challenging problems among environmental technologies [5].

Biosorption has received more attention because of its potential advantages over the traditional methods. Various types of biosorbents such as bacteria, fungi, algae, active sludge, agricultural and industrial wastes have been tested for their biosorption abilities under different experimental conditions [6]. Different agricultural wastes such as peat [7], deoiled soya and rice bran [8], wheat bran [9], skin almond waste [10] and banana peel [11] have been used for biosorption process.

In practice, most industrial effluents contain several dyes. Therefore, it is necessary to study the simultaneous biosorption of two or more dyes from aqueous solutions. One of the problems to be solved in multi-component biosorption is determination of dyes concentration in mixture. UV-Vis spectrometry [12], chromatographic methods [13], capillary electrophoresis [14] and stripping voltammetric techniques [15] are often used to dye analysis. However, these methods often require complicated pretreatment procedures. Spectrophotometric methods are more economic and simpler, but presence of the overlapped

---

*Corresponding author. E-mail: r.tabaraki@ilam.ac.ir

absorption spectra in dye mixture limit the use of traditional spectrophotometric techniques. This problem can be solved by separation steps or chemometrics methods.

Different mathematical methods are used in multivariate data analysis. Data matrix can be reduced by principal component analysis to independent and orthogonal components. Linear and nonlinear methods are also used for modeling. Artificial neural network (ANN) and wavelet neural networks are nonlinear methods. In wavelet neural network, wavelet theory and feed-forward neural network principles are combined. For spectrophotometric determinations, nonlinear modeling systems such as principal component-artificial neural network (PC-ANN) and principal component-wavelet neural network (PC-WNN) have been used [16-18]. The dimensional reduction by principal component analysis (PCA) before model construction has advantages such as increasing stability of model and reducing the amount of co-linearity between variables.

Biosorption factors in a batch system include solution pH, mass of biosorbent, dye concentration, contact time, and solution temperature [19]. Thus, several factors should be optimized. Many statistical experimental design methods have been employed in optimization. Among them, Doehlert designs offer the following advantages: 1) It needs fewer experiments; 2) the number of levels is not the same for all variables, which allows flexibility to assign a large or a small number of levels to the selected variables. Generally it is preferable to choose the variable with the stronger effect as the variable with maximum levels in order to obtain maximum information of the system; 3) Doehlert design is more efficient than central composite design or Box-Behnken design (efficiency of any experimental design is defined as the number of coefficients of the model divided by the number of experiments); 4) Doehlert designs are also more efficient in mapping space: adjoining hexagons can fill a space completely and efficiently, since the hexagons fill space without overlaping [20,21].

In this work, different agriculture wastes are proposed as economical, available and highly effective dye biosorbent. Concentration of each dye in ternary system is determined by principal component-wavelet neural network. Dohelert design and response surface methodology (RSM) are used to optimize the removal of dyes in aqueous solutions. The kinetics, isotherms and thermodynamics of biosorption of these dyes are also evaluated.

EXPERIMENTAL

Reagents, Biosorbent and Instruments

All chemicals including NaOH, HCl, methylene blue (MB), malachite green (MG) and rhodamine B (RB) were obtained from Merck (Darmstadt, Germany). The stock dye solutions were prepared by dissolving an appropriate amount of dye in double distilled water and the desired concentrations of test solutions were prepared by diluting the stock solution. Absorption spectra of MB, RB and MG in single and ternary solutions (initial dye concentration of 10^{-5} M for each dye) are shown in Fig. 1.

Raw pistachio was obtained from the Semnan, Iran. Fruits were manually dehulled and collected hulls were then rinsed with distilled water. The hulls were dried in an oven (Memmert, GmbH + Co. KG, DIN 40050, Germany) with air circulation at 40 ºC, and they were finely ground in a laboratory grinder (Pars Co., Iran). The ground sample was sieved and 0.106-0.250 mm fraction was used for experiments.

The mixture absorption spectra were recorded by UV-Vis spectrophotometer (Varian 300 Bio, Australia) and the pH-meter (Metrohm, model-780, Switzerland, Swiss) was used for pH adjustment. The morphology of the pistachio hull was observed by scanning electron microscopy (SEM) (Hitachi S-4160) under an acceleration voltage of 10 kV.

Determination of the Zero Point Charge pH (pH_{ZPC})

The zero point of charge (pH_{ZPC}) for the pistachio hull was determined by the pH drift method. In this method, the pH was adjusted in the range of 1-7 by addition of HCl and/or NaOH and pistachio hull was added to 50 ml of solution and stirred for 24 h. Difference in final and initial pH of the solution was calculated and plotted against initial solution pH. The surface is neutral when pH = pH_{ZPC}. The surface is negatively charged at pH values greater than pH_{ZPC} and positively charged at pH values lower than pH_{ZPC} [22,23].
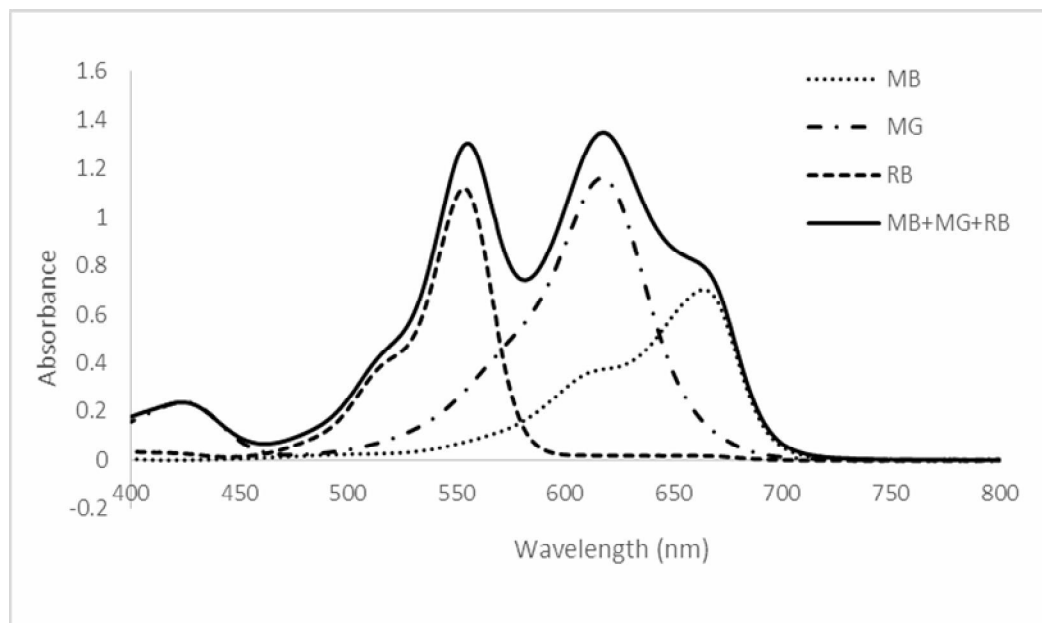
Fig. 1. Absorption spectra of MB, RB and MG in single and ternary solutions (initial dye concentration of 10^{-5} M for each dye).

Table 1. Doehlert Experimental Design

X_1	X_2	X_3	m (g l^{-1})	pH	t (min)	q (mmol g^{-1})
0	0	0	0.25	6.50	40	0.345
0	1	0	0.25	8.00	40	0.431
0.866	0.5	0	0.40	7.25	40	0.544
0.289	0.5	0.816	0.30	7.25	70	0.682
0	-1	0	0.25	5.00	40	0.325
-0.866	-0.5	0	0.10	5.75	40	0.350
0.866	-0.5	0	0.40	5.75	40	0.362
-0.866	0.5	0	0.10	7.25	40	0.349
-0.289	-0.5	-0.816	0.20	5.75	10	0.272
0.289	-0.5	0.816	0.30	5.75	70	0.458
-0.289	0.5	-0.816	0.20	7.25	10	0.282
-0.577	0	0.816	0.15	6.50	70	0.561
0.577	0	-0.816	0.35	6.50	10	0.300

Biosorption Test

The batch sorption experiments were carried out in 100 ml Erlenmeyer flasks, where 0.01-0.04 g of the pistachio hull and 100 ml of the dye solutions (10^{-4} M) were added following pH adjustment. Experimental solutions were obtained by successive dilutions. The pH of the dye solutions was adjusted by NaOH/HCl (0.1 M). The Erlenmeyer flasks were subsequently capped and agitated for 10-70 min at room temperature to achieve equilibrium. At the end of the equilibrium period, the solutions were filtered to separate the pistachio hull and the residual concentrations of MB, MG and RB in the filtrate were quantified by spectrophotometric and chemometrics methods. The data obtained from adsorption tests were used to calculate the adsorption capacity, q_e (mg g^{-1}):

$$q_e = V (C_o - C_e)/m \qquad (1)$$

where C_o and C_e are the initial and equilibrium concentrations of dyes in solution (mM), V is the volume of dye solution (l), q_e is the amount of dyes adsorbed per unit of biosorbent mass (mmol g^{-1}), and m is the mass of biosorbent (g).

Experimental Design and Statistical Analysis

Different operating conditions (pH, biosorbent dosage and time) were optimized using response surface methodology based on a Doehlert experimental design. The levels of the variables were selected according to the preliminary studies. To study the effect of these three variables, Doehlert experimental design based on 13 combinations of the three variables was studied. The equally spaced values of each independent variable and the combination between them were adopted and coded. The interrelationship between dependent and operational variables was established by a model including linear, interaction and quadratic terms. A quadratic polynomial model was constructed for the description of the measured response as functions of the process variables:

$$Y = b_0 + b_1 X_1 + b_2 X_2 + b_3 X_3 + b_{12} X_1 X_2 + b_{13} X_1 X_3 + \\ b_{23} X_2 X_3 + b_{11} X_1^2 + b_{22} X_2^2 + X_3^2 \qquad (2)$$

where X_1, X_2 and X_3 are the values of the three factors (biosorbant dosage, pH and time), expressed as coded variables; b denotes the regression coefficients (calculated from experimental data by the least-squares method) and Y represents the experimental responses measured (q).

The coded and real values are shown in Table 1. Results were analyzed using Minitab 16 (Minitab Inc., State College, PA, USA) software and fitted to a second-order polynomial regression model. The significances of all terms in the polynomial were analyzed statistically by computing the *F*-value at a probability (*p*) of 0.001, 0.01 or 0.05.

Determination of Dye Concentrations in Mixture and Wavelet Neural Network Optimization

To cover the entire dye concentration range and avoid correlation between them, fifty solutions containing different amounts of all three dyes (at pH of 7) were prepared. Concentration of dyes in 50 solutions were 1×10^{-6}-2×10^{-5} M, 1×10^{-6}-1.6×10^{-5} M and 1×10^{-6}-1.6×10^{-5} M for methylene blue, malachite green and rhodamine B, respectively. They were in linear range in calibration curve of each dye. Thirty, ten and ten solutions were used as calibration, prediction and validation sets, respectively. Calibration, prediction and validation sets were used to optimize the network parameters, to prevent over-fitting and evaluation of the performance of the model, respectively.

The absorption spectra of the solutions were recorded from 451 nm to 700 nm in 1 nm intervals. Since 250 data points were recorded for each solution, the response data of the calibration set was a matrix with 30×250 dimensions. The calibration data matrix was subjected to principal component analysis (PCA) using singular value decomposition (SVD). The scores were selected as input nodes in wavelet neural network. The PC-WNN architectures were different for each dye. The number of PCs as an input layer, the number of nodes in hidden layer and other parameters, except the number of iterations, were optimized simultaneously.

Kinetic Experiments

Biosorption kinetic in single and ternary systems were studied in 100 ml Erlenmeyer flasks (dye concentration of 10^{-5} M, biosorbent dosage of 0.5 g l^{-1}, gentle agitation with magnetic stirrer and temperature of 25 °C). The pH was

adjusted to 7 before adding the pistachio hull. At given intervals, samples were taken, filtered, and the filtrate was used to determine dyes concentrations. All of the experiments were carried out three times and the experimental results were expressed as mean.

In order to investigate the kinetic of biosorption, dye biosorption process was analyzed using the pseudo first-order and pseudo-second-order kinetic models [24,25]:

$$ln\ (q_e - q_t) = ln\ q_e - k_1\ t \tag{3}$$

$$\frac{t}{q_t} = \frac{1}{k_2 q_e^2} + \frac{t}{q_e} \tag{4}$$

where k_1 and k_2 show rate constant of the pseudo-first order and pseudo-second-order rate constants, q_t and q_e are the amount of dye adsorbed at time t and saturation (mmol g^{-1}), respectively.

The constant k_2 is used to calculate the initial sorption rate (h) at t→0 as follows:

$$h = k_2 q_e^2 \tag{5}$$

Biosorption Isotherm

In this study, several isotherms (Langmuir, Freundlich, Dubinin-Radushkevich, Redlich-Peterson, Hill, Sips, Koble-Corrigan and Radke-Prausnitz isotherms) were used to correlate the results of dye adsorption by pistachio hull [26]. Nonlinear regression method was used to fit equilibrium biosorption data. It was suggested that fitting of nonlinear models are preferred because linearization of the isotherm equations changes the original error distribution [27]. The adsorption equilibrium data for MB, MG and RB in single and ternary systems by pistachio hull were analyzed by non-linear curve fitting analysis implemented in the Mathematica 8 software.

Langmuir isotherm refers to homogeneous adsorption, in which each molecule possesses constant enthalpies and sorption activation energy, with no transmigration of the adsorbate in the plane of the surface. All sites possess equal affinity for the adsorbate. The Langmuir model is:

$$q_e = \frac{Q_0 K_L C_e}{1 + K_L C_e} \tag{6}$$

where C_e is the equilibrium concentration of adsorbate (mg l^{-1}), q_e denotes the adsorbate adsorbed per gram of the adsorbent at equilibrium (mg g^{-1}), Q_0 represents the monolayer coverage capacity (mg g^{-1}) and K_L is the Langmuir isotherm constant (l mg^{-1}).

Freundlich isotherm describes non-ideal and reversible adsorption, not restricted to the formation of monolayer. This empirical model can be applied to multilayer adsorption, with non-uniform distribution of adsorption heat and affinities over the heterogeneous surface:

$$q_e = K_f C_e^{\frac{1}{n}} \tag{7}$$

where C_e (mg l^{-1}) is the aqueous-phase equilibrium concentration, q_e (mg g^{-1}) is the solid-phase equilibrium concentration, and K_f and n are the Freundlich sorption coefficient and the Freundlich exponent, respectively.

Dubinin-Radushkevich is an empirical model applied to express the adsorption mechanism with a Gaussian energy distribution onto a heterogeneous surface. The Dubinin-Radushkevich equation defined by the following equation:

$$q_e = Q_m \exp\ (-K\varepsilon^2) \tag{8}$$

where K is the Dubinin-Radushkevich isotherm constant related to the adsorption energy (mol^2 kJ^{-2}), Q_m is the theoretical isotherm saturation capacity (mg g^{-1}), ε is the Polanyi potential, calculated from Eq. (9):

$$\varepsilon = RT \ln(1 + \frac{1}{C_e}) \tag{9}$$

Redlich-Peterson isotherm is a hybrid isotherm featuring both Langmuir and Freundlich isotherms incorporating three parameters into an impirical equation. It represents adsorption equilibrium over a wide concentration range that can be applied either in homogeneous or heterogeneous systems due to its versatility:

$$q_e = \frac{K_{RP} C_e}{1 + a_{RP} C_e^g} \tag{10}$$

where K_{RP} is the Redlich-Peterson model isotherm constant

(l g^{-1}), a$_{RP}$ is the Redlich-Peterson model constant (mg l^{-1}); g is the Redlich-Peterson model exponent.

Hill isotherm was used to describe the binding of different species onto homogeneous substrates assuming that adsorption is a cooperative phenomenon, with the ligand binding ability at one site on the macromolecule, that may influence different binding sites on the same macromolecule:

$$q_e = \frac{q_{sH} C_e^{n_H}}{K_D + C_e^{n_H}} \qquad (11)$$

where q_{sH} is the Hill isotherm maximum uptake saturation (mg l^{-1}), K$_D$ is the Hill constant, n$_H$ is the Hill cooperativity coefficient of the binding interaction.

By identifying the problem of continuing increase in the adsorbed amount with an increase in concentration in the Freundlich equation, Sips proposed an equation similar in form to the Freundlich equation, but it has a finite limit when the concentration is sufficiently high:

$$q_e = \frac{q_{ms} K_s C_e^{ms}}{1 + K_s C_e^{ms}} \qquad (12)$$

where q$_{ms}$ is the Sips maximum adsorption capacity (mg/g), K$_s$ is the Sips equilibrium constant (l mg^{-1})^{ms} and m$_s$ is the Sips model exponent, limited from 0 to 1.

Koble-Corrigan model is the three-parameter empirical model based on the combination of both the Langmuir and Freundlich isotherm equations representing in one non-linear equation of the equilibrium adsorption data. The model is commonly expressed by Eq. (13):

$$q_e = \frac{a C_e^n}{1 + b C_e^n} \qquad (13)$$

where a (l^n mg^{1-n} g^{-1}), b (l mg^{-1})^n and n are the Koble-Corrigan parameters. This model is generally applied for heterogeneous sorbent surface.

The three isotherms of Radke and Prausnitz model can be represented as:

$$q_e = \frac{q_{m_{RPII}} K_{RPII} C_e}{1 + K_{RPII} C_e^{m_{RPII}}} \qquad (14)$$

$$q_e = \frac{q_{m_{RPIII}} K_{RPIII} C_e^{m_{RPIII}}}{1 + K_{RPII} C_e^{m_{RPIII}-1}} \qquad (15)$$

where q$_{mRPI}$, q$_{mRPII}$ and q$_{mRPIII}$ are the Radke-Prausnitz maximum adsorption capacities (mg g^{-1}), K$_{RPI}$, K$_{RPII}$ and K$_{RPIII}$ are the Radke-Prausnitz equilibrium constants, and m$_{RPI}$, m$_{RPII}$ and m$_{RPIII}$ are the Radke-Prausnitz model exponents [26,28].

An error function is defined to enable the optimization process to determine and evaluate the fit of the isotherm equation to the experimental data. In the current work, several mathematically rigorous error functions were examined. Error functions were discussed in detail in Rangabhashiyam paper [28].

Thermodynamic Study

Temperature effects were investigated at three different temperatures 20, 30, 40 and 50 °C. For this purpose, dried biomass was added to 250 ml dye solution in 500-ml Erlenmeyer flasks (each dye concentration of 10^{-5} M, biosorbent dosage of 0.3 g l^{-1} and pH = 7.25). The flasks were placed in a thermostatic water bath on a shaker with constant shaking. After 70 min, the concentrations of each dye in the filtrates were determined. The value C$_{ad,eq}$ (mM) is the amount of each dye on the biosorbent at equilibrium and C$_{eq}$ (mM) is the dye concentration remaining in solution at equilibrium conditions. The C$_{ad, eq}$ was determined as the difference of initial and remaining dye concentration in solution at equilibrium conditions. These concentrations were used for calculation of the equilibrium constant (K$_C$ = C$_{ad,eq}$/C$_{eq}$).

RESULTS AND DISCUSSION

Biosorbent

Pistachio hull was selected as a biosorbent model for the removal of three dyes (MB, MG and RB). The pistachio hull was analyzed by scanning electron microscopy to examine its textural structure. A SEM micrograph of unloaded biomass shown in Fig. 2a indicates the porous structure of the biomass. Figure 2b shows a SEM micrograph of the biomass loaded with dyes. The biomass structure changed after biosorption of the dyes and had a
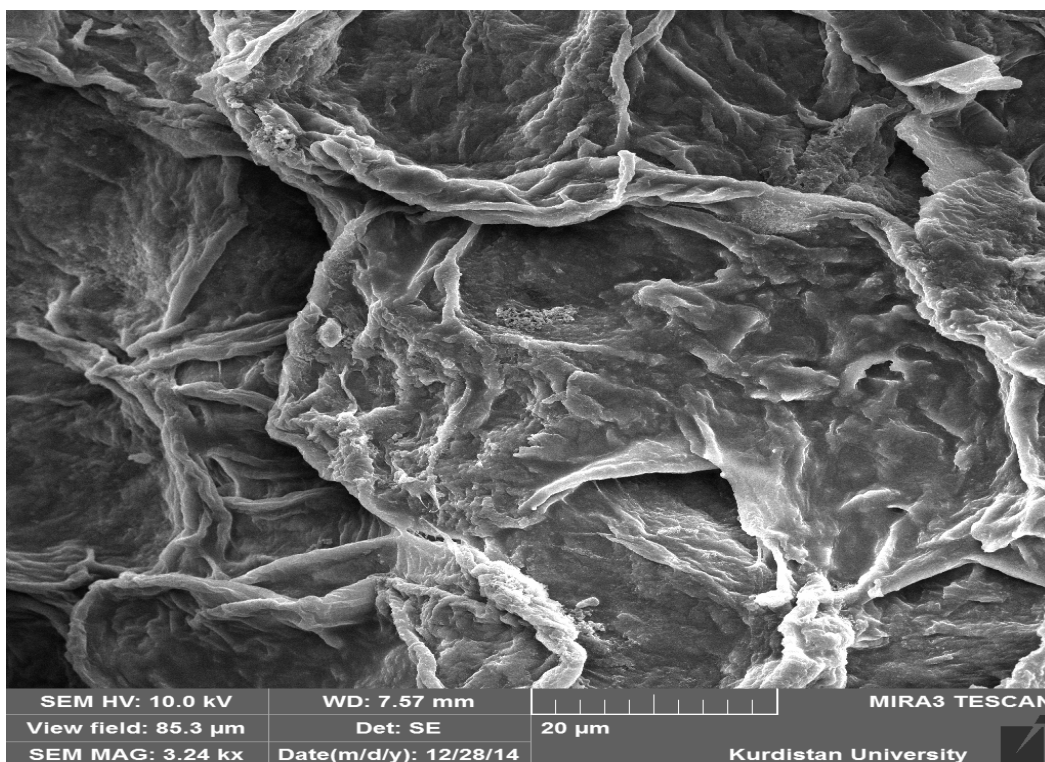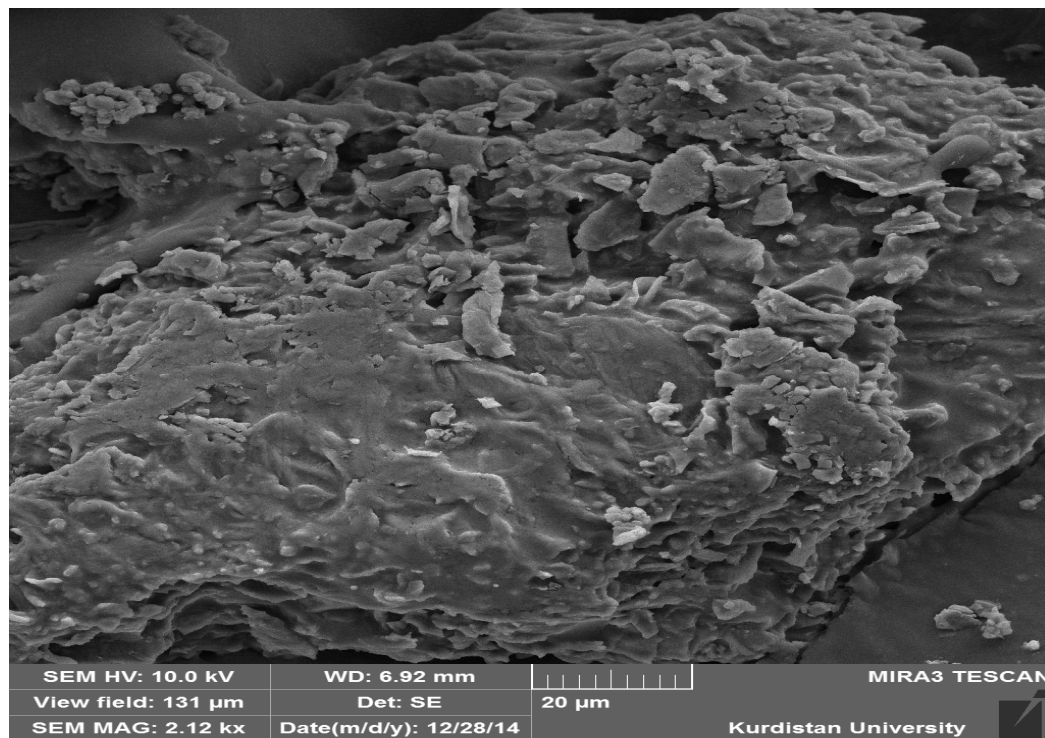
Fig. 2. (a) SEM of pistachio hull before biosorption. (b) SEM of same pistachio hull after multi dyes adsorption.
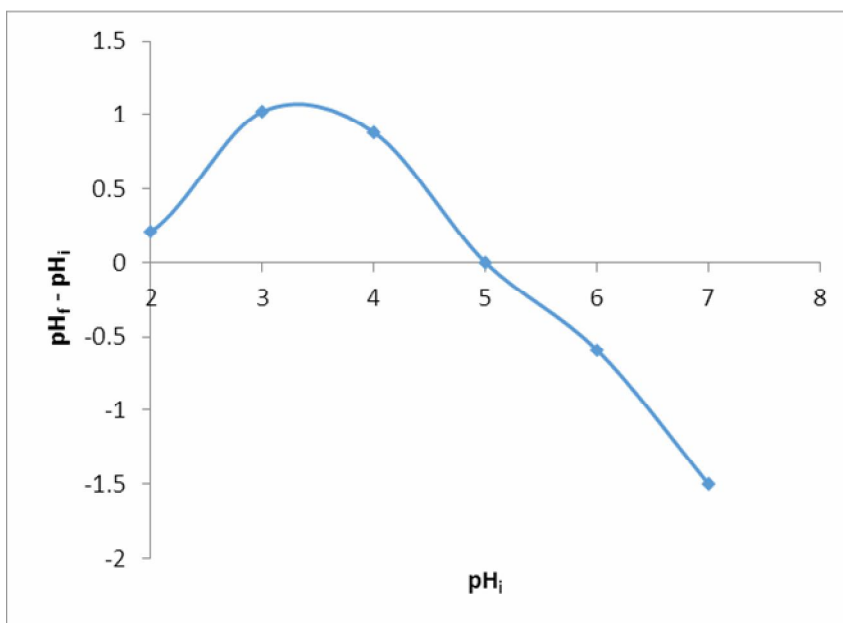
Fig. 3. The point of zero charge (pH_{zpc}).

tendency to form agglomerates.

Biosorption in a Single System

    Effect of pH. At low pH, as a result of protonation of the functional groups, surface gets positively charged and the strong repulsive forces between the cationic molecules and surface lead to significant decrease in the dye removal. The increase in the initial pH lead to deprotonation of the active adsorption sites on surface and electrostatic interaction and/or hydrogen bonding adsorbs the dye molecule. The pH_{ZPC} value of the pistachio hull was found to be 5.0. The surface of the pistachio hull is neutral when pH of the aqueous solution is equal to pH_{ZPC} (Fig. 3). At pH > pH_{PZC}, the adsorbent surface is negatively charged due to deprotonation of its functional group that causes an increase in the adsorption percentage.

    The initial pH of the aqueous solution affects dye aqueous chemistry and surface binding sites of the biosorbents. Generally, a shift in UV-Vis spectra of dyes or a change in absorbance is associated with a wide change in pH. In single dye systems, different calibrations were prepared for each pH. The effect of initial pH on the MB, MG and RB removal was studied in the pH range of 2-8 with initial dye concentration of 10^{-5} M and biosorbent dose

of 0.05 g. The experiments were conducted for 30 min of contact time at room temperature and the respective results are presented in Fig. 4a. The initial pH significantly affects the extent of biosorption of MB, MG and RB on the pistachio hull and the maximum uptake is significantly increased at higher pH values. As can be seen, the maximum uptake of MB, MG and RB is highest at pH values of 7.0, 5.0 and 5.0, respectively.

    Effect of biosorbent dose. The maximum uptake of MB, MG and RB decreases with increase in biosorbant dose (Fig. 4b). At constant dye concentration, dye removal capacity decreased by biosorbent dose increase (due to increase in biosorbent mass, Eq. (1)). The sorption of Direct Blue 71 by wheat shells from aqueous solution occurred at low biosorbent doses [29]. Similar behavior on peanut hull was observed [30].

    Effect of time. Equilibrium time is one of the most important parameters in the design of economical wastewater treatment systems. In order to determine the biosorption equilibrium time for MB, MG and RB dyes, the contact time was varied from 2 to 70 min at room temperature and total concentration of 10^{-5} M. The pH was adjusted at 6 and 100 ml of sample solution was stirred with 0.05 g of adsorbent. The results were shown in Fig. 4c and it
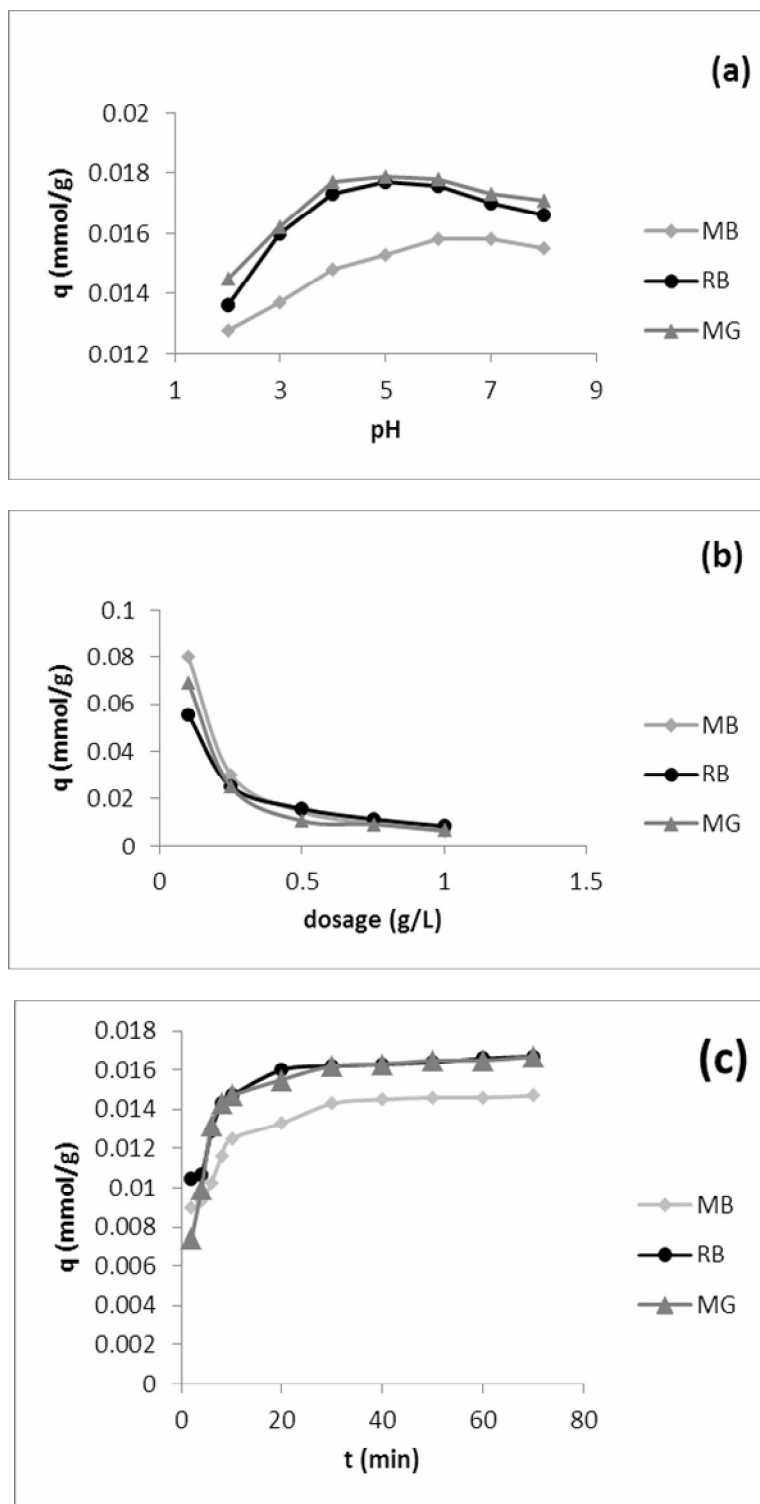
Fig. 4. (a) Effect of pH on biosorption of MB, RB and MG onto pistachio hull, (b) effect of biomass dosage, (c) effect of contact time (dye concentration: 10^{-5} M; pH: 6; biomass dosage: 0.5 g l^{-1}; time: 30 min).

Table 2. The Optimized Parameters of PC-WNN Models

Parameters	RB	MB	MG
Input neurons	3	3	3
Hidden neurons	2	2	2
Output neurons	1	1	1
Learning rate	0.058	0.067	0.051
Momentum	0.87	0.22	0.20
Number of iterations	1000	3000	2000
Hidden transfer function	Morlet	Morlet	Morlet
Output transfer function	Linear	Linear	Linear

Table 3. First-order and Second-order Kinetic Constants of MB, MG and RB Dyes in Single and Ternary Systems

System	Dye	Pseudo-first-order			Pseudo-second-order			
		K_1	q_{e1}	R^2	K_2	q_{e2}	R^2	q_{exp}
Single	MB	0.1374	0.0083	0.876	27.03	0.017	0.999	0.0162
	MG	0.099	0.0065	0.936	29.41	0.015	0.999	0.0143
	RB	0.1933	0.0099	0.989	34.48	0.017	0.999	0.0162
Ternary	MB	0.0574	0.0066	0.989	15.15	0.011	0.996	0.0098
	MG	0.0384	0.006	0.915	21.28	0.012	0.994	0.0114
	RB	0.0454	0.0064	0.900	21.27	0.013	0.996	0.0129

is observed that MB, MG and RB biosorption on pistachio hull occurs relatively rapid and approaches to equilibrium within 30 min at room temperature [31].

Determination of Dye Concentration in a Ternary System and an Experimental Design

Figure 1 shows absorbance spectra of the single and ternary solutions of MB, MG and RB (10^{-5} M for each dye). The simplest and the most common method is a top-down variable selection where the PCs are ranked in the order of decreasing eigenvalue. The PC with the highest eigenvalue is considered as the most significant one, and, subsequently, the PCs are introduced into the WNN model one after the other. WNN models were developed using different numbers of the PCs in input layer. The WNN variables consisted of the number of PCs as an input layer, the number of nodes in the hidden layer, the learning rate, the momentum and the number of epochs, which optimized for each dye separately. The optimized variable parameters for each dye are given in Table 2.

Table 4. Comparison of Different Isotherms Based on Error Functions

Model	Single			Ternary		
	MB	MG	RB	MB	MG	RB
Langmuir						
SSE	4.6×10^{-5}	3.11×10^{-5}	1.32×10^{-4}	9.95×10^{-5}	7.65×10^{-5}	1.82×10^{-5}
ARE	16.19	5.32	80.56	38.09	133.46	10.07
R^2_{adj}	0.9954	0.9858	0.959	0.9653	0.942	0.9863
Freunndlich						
SSE	3.71×10^{-4}	2.06×10^{-4}	3.58×10^{-4}	2.09×10^{-4}	1.57×10^{-4}	1.72×10^{-5}
ARE	64.43	16.34	210.13	86.24	281.09	16.03
R^2_{adj}	0.963	0.9062	0.8883	0.927	0.8809	0.9871
Dubinin-Radushkevich						
SSE	5.93×10^{-5}	5.63×10^{-5}	1.88×10^{-4}	1.05×10^{-4}	9.22×10^{-5}	1.87×10^{-5}
ARE	6.82	7.19	89.49	23.48	114.36	11.8
R^2_{adj}	0.9941	0.9743	0.9413	0.9633	0.9302	0.9859
Redlich-Peterson						
SSE	1.46×10^{-6}	1.78×10^{-5}	1.78×10^{-5}	1.11×10^{-5}	1.02×10^{-5}	1.44×10^{-5}
ARE	5.34	3.55	43.57	14.9	78.74	6.51
R^2_{adj}	0.9999	0.9909	0.9942	0.9959	0.9918	0.9871
Hill						
SSE	3.14×10^{-6}	2.1×10^{-5}	5.6×10^{-5}	1.93×10^{-5}	1.57×10^{-4}	1.39×10^{-5}
ARE	5.46	3.35	8.6819	24.27	281.09	8.76
R^2_{adj}	0.9997	0.9892	0.9818	0.9928	0.8729	0.9891
Sips						
SSE	3.14×10^{-6}	2.1×10^{-5}	4.83×10^{-5}	1.93×10^{-5}	1.49×10^{-5}	1.39×10^{-5}
ARE	5.48	3.35	9.07	24.27	18.86	8.76
R^2_{adj}	0.9997	0.9892	0.9843	0.9928	0.9879	0.9891
Koble-Corrigan						
SSE	3.14×10^{-6}	2.1×10^{-5}	4.83×10^{-5}	1.93×10^{-5}	1.49×10^{-5}	1.39×10^{-5}
ARE	5.48	3.35	9.07	24.27	18.86	8.76
R^2_{adj}	0.9997	0.9892	0.9843	0.9928	0.9879	0.9891
Radke-Prausnitz(II)						
SSE	1.46×10^{-6}	2.75×10^{-4}	1.83×10^{-4}	2.2×10^{-5}	1.22×10^{-4}	1.44×10^{-5}
ARE	5.34	14.81	58.28	19.18	108.45	6.51
R^2_{adj}	0.9998	0.8588	0.9907	0.9918	0.9012	0.9887
Radke-Prausnitz(III)						
SSE	1.46×10^{-6}	1.78×10^{-5}	1.78×10^{-5}	1.11×10^{-5}	1.02×10^{-5}	1.44×10^{-5}
ARE	5.34	3.55	43.57	14.91	78.74	6.51
R^2_{adj}	0.9998	0.9909	0.9942	0.9959	0.9918	0.9910

SSE: Sum squares errors, ARE: Average relative error, R_{adj}^2: Adjusted determination coefficient.

Table 5. Thermodynamic Parameters for Biosorption of MB, MG and RB in Single and Ternary Systems

	Dye	T	ΔG^o	ΔH^o	ΔS^o
		(K)	(kJ mol^{-1})	(kJ mol^{-1})	(J mol^{-1})
Single	MB	293	-8.28	12.69	72.4
		303	-9.6		
		313	-10		
		323	-10.56		
	MG	293	-8.95	12.5	39.4
		303	-9.38		
		313	-9.81		
		323	-10.12		
	RB	293	-7.33	10.63	60.8
		303	-7.66		
		313	-8.25		
		323	-9.16		
Ternary	MB	293	-6.13	5.29	39
		303	-6.41		
		313	-6.77		
		323	-7.45		
	MG	293	-6.35	8.94	51.8
		303	-6.6		
		313	-7.22		
		323	-7.87		
	RB	293	-6.67	9.71	55.7
		303	-7.06		
		313	-7.67		
		323	-8.32		

A surface response methodology based on a Doehlert experimental design was applied to study the effects of pH, biosorbent concentration and time on biosorption capacity of dye (MB, MG and MB) in ternary system (Table 1). A full quadratic model containing ten coefficients was used to describe the response observed to fit Eq. (2). Second-order polynomial model for q (mmol g^{-1}) was:

q (mmol g^{-1}) = 0.345 + 0.043 X_1* + 0.078 X_2* + 0.141 X_3* + 0.048 X_1^2 + 0.033 X_2^2 + 0.065 X_3^2 + 0.092 $X_1 X_2$* + 0.0006 $X_1 X_3$ + 0.077 $X_2 X_3$

$R^2 = 0.977$ (16)

The significances of all terms were analyzed statistically by computing the *F*-value at a probability (*p*) of 0.05 and significant terms identified by star. It is important to find out the optimal conditions using developed mathematical model. The optimized conditions were initial solution pH 7.25, contact time 70 min and adsorbent dosage 0.3 g l^{-1}. At this condition, biosorption capacity was 0.682 mmol g^{-1}.

Kinetic Modeling

Table 3 lists pseudo first-order and pseudo second-order rate constants for MB, MG and RB in single as well as ternary systems. The correlation coefficient (R^2) for the pseudo second-order adsorption model was relatively high, and the adsorption capacities calculated by the model were also close to those determined by experiments. However, the values of R^2 for the pseudo first-order model were not satisfactory. Therefore, it has been concluded that the pseudo second-order adsorption model was more suitable to describe the biosorption kinetics of MB, MG and RB.

In addition, the initial bisorption rate, h = $k_2 q_e^2$, has been widely used for evaluation of the biosorption rates [32]. In the present study, the values of initial bisorption rate decreased as follows: 0.01 mmol g^{-1} min^{-1} RB > 0.008 mmol g^{-1} min^{-1} MB > 0.0067 mmol g^{-1} min^{-1} MG > 0.0038 mmol g^{-1} min^{-1} RB (MB-MG-RB) > 0.0029 mmol g^{-1} min^{-1} MG (MB-MG-RB) > 0.0017 mmol g^{-1} min^{-1} MB (MB-MG-RB) indicating that pistachio hull can adsorb RB more rapidly than MB and MG from aqueous solutions. The overall order of biosorption is dependent upon the

characteristics of the dyes as well as the nature of biosorbent.

Biosorption Isotherm Models

The adsorption equilibrium data for MB, MG and RB in single and ternary systems were analyzed by non-linear curve fitting analysis for two-parameter (Langmuir, Freundlich and Dubinin-Radushkevich) and three-parameter (Redlich-Peterson, Hill, Sips, Koble-Corrigan and Radke-Prausnitz) isotherm models. Table 4 shows the values of average relative error (ARE), sum of squares or the error (SSE), and adjusted determination coefficient (R_{adj}^2) used to check the validity of the isotherm models. It was concluded that the three-parameter models of Redlich-Peterson and Radke-Prausnitz had the best correlation.

Thermodynamic Study

The value of thermodynamic parameters (free energy, enthalpy and entropy changes) as criterion for evaluation of feasibility and the spontaneous nature of the process were evaluated from the following equation [33]:

$$\Delta G° = -RT \ln K_C$$ (17)

where $\Delta G°$, R, K_C and T are the free energy change (kJ mol^{-1}), universal gas constant (8.314 J mol^{-1} K^{-1}), equilibrium constant and absolute temperature (K), respectively. The slope and intercept of Van't Hoff plot (ln K_D *vs.* 1/T) were used to evaluate $\Delta H°$ and $\Delta S°$:

$$\ln K_c = \frac{\Delta S°}{R} - \frac{\Delta H°}{RT}$$ (18)

where R is the universal gas constant (8.314 J mol^{-1} K^{-1}), K_C, the thermodynamic equilibrium constant and T is the absolute temperature (K). The thermodynamic parameters (Table 5) such as negative $\Delta G°$ values confirm the spontaneous nature and feasibility of the adsorption process. The positive value of ΔH strongly supports the endothermic nature of adsorption while the positive value of ΔS shows the increase in randomness at the solid/solution interface during the adsorption of MB, MG and RB on pistachio hull.

CONCLUSIONS

Some crucial implications of this study are listed below:

1. Multivariate analysis methods such as principal component-wavelet neural network were successfully used for determination of dyes with overlapped spectra in ternary solutions.

2. In single and ternary systems, the Redlich-Peterson and Radke-Prausnitz models showed a better fit with the following sorption order: RB > MG > MB.

3. The biosorption performance of pistachio hull for dyes was fairly good with biosorption capacity of 0.682 mmol g^{-1}.

4. Thermodynamically, the biosorption of MB, MG, RB dyes by pistachio hull from single and ternary solutions was spontaneous ($\Delta G° < 0$) and endothermic ($\Delta H° > 0$) with high preference of dyes towards the biomass surface ($\Delta S° > 0$).

ACKNOWLEDGEMENTS

REFERENCES

[1] F.C. Wu, R.L. Tseng, J. Hazard. Mater. 152 (2008) 1256.

[2] M. Arami, N.Y. Limaee, N.M. Mahmoodi, N.S. Tabrizi, J. Hazard. Mater. 135 (2006) 171.

[3] L. Brinza, C.A. Nygard, M.J. Dring, M. Gavrilescu, L.G. Benning. Bioresour. Technol. 100 (2009) 1727.

[4] V. Vimonses, B. Jin, C.W.K. Chow. J. Hazard. Mater. 157 (2010) 472.

[5] A.N. Soon, B.H. Hameed. Desalination 269 (2011) 1.

[6] T. Akar, S. Arslan, S.T. Akar. Ecol. Eng. 58 (2013) 363.

[7] S.J. Allen, G. Mckay, J.F. Porter. J. Colloid Interf. Sci. 280 (2004) 322.

[8] A. Mittal, J. Mittal, A. Malviya, D. Kaur, V.K. Gupta, J. Colloid Interf. Sci. 343 (2010) 463.

[9] X.S. Wang, X. Liu, L. Wen, Y. Zhou, Y. Jiang, Z. Li, Sep. Sci. Technol. 43 (2008) 3712.

[10] F. Atmani, A. Bensmaili, N.Y. Mezenner, J. Environ. Sci. Technol. 2 (2009) 153.

[11] K. Amel, M.A. Hassena, D. Kerroum, Energy Procedia 19 (2012) 286.

[12] F. Sánchez Rojas, C. Bosch Ojeda, Anal. Chim. Acta 635 (2009) 22.

[13] M. Kucharska, J. Grabka, Talanta 80 (2010) 1045.

[14] A. Peláez-Cid, S. Blasco-Sancho, F. Matysik, Talanta 75 (2008) 1362.

[15] A.H. Alghamdi, Arabian J. Chem. 3 (2010) 1.

[16] A.A. Ensafi, T. Khayamian, R. Tabaraki, Talanta 71 (2007) 2021.

[17] P.J. Gemperline, J.R. Long, V.G. Gregoriou, Anal. Chem. 63 (1991) 2313

[18] T. Khayamian, A.A. Ensafi, R. Tabaraki, M. Esteki. Anal. Lett. 38 (2005) 1477.

[19] E.C. Lima, B. Royer, J.C.P. Vaghetti, J.L. Brasil, N.M. Simon, A.A. dos Santos Jr, F.A. Pavan, S.L.P. Dias, E.V. Benvenutti, E.A. da Silva, J. Hazard. Mater. 140 (2007) 211.

[20] S.L.C. Ferreira, W.N.L. dos Santos, C.M. Quintella, B.B. Neto, J.M. Bosque-Sendra, Talanta 63 (2004) 1061.

[21] P. Vanloot, J.L. Boudenne, L. Vassalo, M. Sergent, B. Coulomb, Talanta 73 (2007) 237.

[22] E. Kiefer, L. Sigg, P. Schosseler, Environ. Sci. Technol. 31 (1997) 759.

[23] B.K. Nandi, A. Goswami, M.K. Purkait, J. Hazard. Mater. 161 (2009) 387.

[24] T.K. Sen, S. Afroze, H.M. Ang, Water Air Soil Pollut. 218 (2011) 499.

[25] M. Mohammad, S. Maitra, N. Ahmad, A. Bustam, T.K. Sen, B.K. Dutta, J. Hazard. Mater. 179 (2010) 363.

[26] K.Y. Foo, B.H. Hameed, Chem. Eng. J. 156 (2010) 2.

[27] Y.S. Ho, W.T. Chiu, C.C. Wang, Bioresour. Technol. 96 (2005) 1285.

[28] S. Rangabhashiyam, N. Anu, M.S. Giri Nandagopal, N. Selvaraju, J. Environ. Chem. Eng. 2 (2014) 398.

[29] Y. Bulut, N. Gozubenli, H. Aydin, J. Hazard. Mater. 144 (2007) 300.

[30] R. Gong, Y. Sun, J. Chen, H. Liu, G. Yang, Dyes Pigments 67 (2005) 175.

[31] J.F. Gao, Q. Zhang, K. Su, J.H. Wang, Bioresour. Technol. 101 (2010) 5793.

[32] S. Dawood, T. Kanti Sen, Water Res. 46 (2012) 1933.

[33] S. Rengaraj, Y. Kim, C.K. Joo, J. Colloid Interf. Sci. 273 (2004) 14.